

Cellular automata simulating experimental properties of traffic flow

Dirk Helbing¹ and Michael Schreckenberg²

¹*II. Institute of Theoretical Physics, University of Stuttgart, Pfaffenwaldring 57/III, 70550 Stuttgart, Germany*

²*Theoretische Physik, Gerhard-Mercator-Universität Duisburg, Lotharstraße 1, 47048 Duisburg, Germany*

(Received 28 January 1998; Revised manuscript received 17 December 1998)

A model for one-dimensional traffic flow is developed, which is discrete in space and time. Like the cellular automaton model by Nagel and Schreckenberg [J. Phys. I **2**, 2221 (1992)], it is simple, fast, and can describe stop-and-go traffic. Due to its relation to the optimal velocity model by Bando *et al.* [Phys. Rev. E **51**, 1035 (1995)], its instability mechanism is of deterministic nature. The model can be easily calibrated to empirical data and displays the experimental features of traffic data recently reported by Kerner and Rehborn [Phys. Rev. E **53**, R1297 (1996)]. [S1063-651X(99)51103-3]

PACS number(s): 05.50.+q, 05.40.-a, 47.55.-t, 89.40.+k

Cellular automata (CA) are interesting for their speed and their complex dynamical behavior [1], including such fascinating phenomena as self-organized criticality [2–4], formation of spiral patterns [5], or oscillatory and chaotic sequences of states [1,5,6]. Their enormous computation speed and efficiency is a consequence of the following properties, which are ideal preconditions for parallel computing: (i) discretization of space into identical sites x , (ii) a finite number of possible states $f(x)$, (iii) the (parallel) update at times $T = t\Delta T$ with an elementary time step ΔT , (iv) globally applied update rules, based on (v) short-range interactions with a finite (small) number of neighboring sites. Despite these simplifications, cellular automata have a broad range of applications, reaching from realistic simulations of granular media [7] or fluids [8] (including interfacial phenomena and magnetohydrodynamics), over the computation of chemical reactions [5,9], up to the modeling of avalanches [3]. Their application to traffic dynamics [10,11] has stimulated an enormous research activity [12–14], aiming at an understanding and control of traffic instabilities, which are responsible for stop-and-go traffic and congestion, both on “free-ways” and in cities.

Recently, Kerner and Rehborn [15] have reported some characteristic properties of empirical highway traffic flow, which a realistic traffic model should display: (i) At small densities, traffic flow is stable, i.e., arbitrarily large disturbances of homogeneous traffic will disappear in the course of time. (ii) Above a certain critical density, any small perturbation will give rise to the formation of a traffic jam. (iii) Between the stable and the unstable regions, there exists a density interval beginning at about 20 vehicles per kilometer, where traffic flow is metastable. That is, sufficiently small disturbances (so-called “subcritical perturbations”) will fade away, whereas “supercritical” perturbations exceeding a certain minimal amplitude will cause a traffic jam. (iv) The outflow from traffic jams has a typical value that is independent of the initial conditions and, to a large extent, independent of the average surrounding traffic density. It varies only with road or weather conditions, and the average vehicle characteristics (regarding their lengths and acceleration capabilities). (v) The typical outflow is considerably smaller than the maximum flow and lies at about 1600 vehicles/km for slow lanes, and on fast lanes between 1800 vehicles/km

(measured in Germany [15]) and 2100 vehicles/km (on Dutch motorways [12]). It is associated with a density of 20 ± 5 vehicles per kilometer. (vi) Downstream jam fronts move with a velocity of -15 ± 5 km/h. Notice that properties (iv) and (vi) originate from the uniform acceleration behavior of queued vehicles, resulting from the similar distances and velocities that they share inside traffic jams. While the propagation velocity C of traffic jams is given by the dissolution speed of a jam front, the outflow Q_{out} is related to the time gap \mathcal{T} between successive departures from the traffic jam [16].

The cellular automaton proposed by Nagel and Schreckenberg [10] meets the properties (i), (ii), and (vi), and most of the other properties can be reproduced by separate variants of it [17–19]. In particular, the continuous version by Krauß *et al.* [18] and the CA by Barlovic *et al.* [19] seem to display metastable states. Moreover, the continuous version is in good agreement with empirical traffic data [18]. Here, we will present a “unifying” cellular automaton which, in a certain parameter range, reproduces all of the above properties. Remarkably, the characteristic quantities can be calculated analytically. Moreover, consistent with *macroscopic* traffic models, the mechanism of traffic jam formation is deterministic [20,13] rather than based on internal fluctuations (“randomization”) [18]. Being related to the optimal velocity model [21], it originates from the delayed adaptation to an equilibrium velocity, which, in the instability region, rapidly decays with growing density [13,20].

We propose the following simple and fast discrete model that can be well calibrated to macroscopic traffic data: To maximize simulation speed, we first choose the time step ΔT of the temporal update as large as possible. It is limited to $\Delta T \approx 1$ s, since this corresponds to the safe time headway required for avoiding accidents. The spatial discretization ΔX of the road should not be larger than the minimal vehicle distance ℓ . A fine velocity discretization $\Delta V = \Delta X / \Delta T$ is reached by taking a fraction $\Delta X = \ell / n$ of ℓ ($n \in \{1, 2, 3, \dots\}$). Velocity steps of the order 5–10 km/h require $\Delta X \leq \ell / 2$. In the following, the spatial coordinate $X = x \Delta X$ and distances $D = d \Delta X$ are measured in units of ΔX , time $T = t \Delta T$ in units of ΔT , and any velocity in units of ΔV .

Assume we want to distinguish A different vehicle types $a \in \{1, 2, \dots, A\}$, e.g., cars and trucks [22]. Then, at each time

$t \in \{0, 1, 2, \dots\}$, every site $x \in \{1, 2, \dots, l\}$ can be in one of the states $f_t(x) = (a, v)$, where $f_t(x) = (0, 0)$ corresponds to an empty site, and $f_t(x) = (a, v)$ with $a > 0$ represents a vehicle of type a with velocity $v \in \{0, 1, 2, \dots, v_{\max}^a\}$. For safety reasons, the velocity v_t must be smaller than the distance d_t to the vehicle ahead. The states of the cellular automaton are updated in parallel according to the following successive steps: First, each vehicle is moved by its actual velocity v_t to position $x + v_t$, which means $f_{t+1}(x + v_t) = f_t(x)$, if $a > 0$ and $v_t > 0$. Then, the states of the previously occupied positions are reset to $f_{t+1}(x) = (0, 0)$. Any other site keeps its previous state. Finally, all vehicle velocities are modified along with the proposed acceleration rule

$$v'_{t+1} = v_t + [\lambda_a [v_a(d_{t+1}) - v_t]], \quad (1)$$

$$v_{t+1} = v'_{t+1} - \begin{cases} 1 & \text{with probability } p, \text{ if } v'_{t+1} > 0 \\ 0 & \text{otherwise,} \end{cases} \quad (2)$$

where $[y]$ is defined by the largest integer $i \leq y$. Therefore, the above equation implies $v_{t+1} \leq \lambda_a v_a(d_{t+1}) + (1 - \lambda_a)v_t$, meaning that the new velocity is a weighted average of the previous velocity v_t and the optimal velocity v_a of vehicle type a , or somewhat less. A small value of the model parameter $\lambda_a \geq 0$ relates to a great inertia of vehicle motion, whereas a large value $\lambda_a \leq 1$ implies a fast adaptation to the distance-dependent optimal velocity $v_a(d)$. The corresponding adaptation time is $\tau_a = \Delta T / \lambda_a$. If the (back-bumper-to-back-bumper) distance d_{t+1} to the next vehicle exceeds a certain finite value d_{fin} , the vehicles do not interact, and v_a is given by the maximum velocity v_{\max}^a of vehicle type a . For small distances v_a should be determined by the velocity-dependent safe distance $d(v_a) \approx \ell / \Delta X + v_a$, required to avoid accidents. The model parameter (“slowdown probability”) p describes individual velocity fluctuations due to delayed acceleration (imperfect driving). Here, we are interested in the limit $p \rightarrow 0$.

In order to compare this discrete model with the observed properties of traffic flows, it is necessary to investigate aggregate quantities $\langle h \rangle$. These are defined by

$$\langle h \rangle_{x,t} = \frac{1}{\Delta t} \sum_{t'=t}^{t+\Delta t-1} \frac{1}{2\Delta x+1} \sum_{x'=x-\Delta x}^{x+\Delta x} h[f_{t'}(x')] \quad (3)$$

The vehicle density is given by $\rho(x\Delta X, t\Delta T) = \langle \Theta(a) \rangle / \Delta X$, the traffic flow by $Q(x\Delta X, t\Delta T) = \langle v \Theta(a) \rangle / \Delta T$, and the average velocity by $V(x\Delta X, t\Delta T) = Q(x\Delta X, t\Delta T) / \rho(x\Delta X, t\Delta T)$, where $\Theta(a) = 1$ for $a \geq 0$, otherwise $= 0$. During the simulation runs, the density minima and maxima, their propagation speed, and the associated traffic flows were evaluated automatically, as well as the spatially averaged vehicle velocity and traffic flow on the circular road of length $L = 20$ km. The corresponding values were averaged over several hours after a sufficiently long transient period. Averages over the whole street are indicated by an overbar.

First, let us discuss the case of one type $a = 1$ of vehicles. Our simulation results can be summarized as follows: At small average densities $\bar{\rho}$, homogeneous traffic flow is stable, and the spatially averaged velocity \bar{V} is given by the

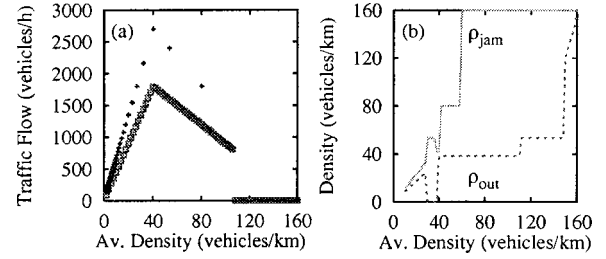


FIG. 1. Simulation results for $v_1(d) = \min(d-1, 3)$, $\lambda_1 = 0.77$, $\Delta T = 1$ s, $\Delta X = 6.25$ m, and (a) $p = 0.001$, (b) $p = 0$, $w_+ = w_- = 200$ m, and $\Delta \rho = \rho/2$. Illustration (a) shows the “optimal flow” $\bar{\rho} v_1(1/\bar{\rho})$ (+) and the resulting average flow $\bar{Q}(\bar{\rho})$ (\square) as a function of the average density $\bar{\rho}$, (b) the densities inside (—) and in front of (---) traffic jams.

density-independent value $(v_1^{\max} - [1/\lambda_1 - 1] - p)\Delta V$. It is zero for high densities [Fig. 1(a)], since $\lambda_1 v_1(d) > 1$ is necessary for the acceleration of a vehicle from standstill.

At medium densities, the resulting velocity-density relation is largely dependent on λ_1 : Regime I: For $1 \geq \lambda_1 \geq \lambda_{\text{stab}}(v_{\max}^1, p)$ (corresponding to a quasi-instantaneous adaptation to the optimal velocity), $\bar{V}(\bar{\rho})$ is close to the piecewise constant relation $v_1(1/\bar{\rho})$. Accordingly, the associated average traffic flow \bar{Q} is a piecewise linear function of $\bar{\rho}$. Regime II: In a certain interval $\lambda_{\min}(v_{\max}^1, p) \leq \lambda_1 \leq \lambda_{\max}(v_{\max}^1, p)$, traffic flow is unstable for a certain range $\rho_{\text{out}} \leq \bar{\rho} \leq \rho_{\text{max}}$ of medium densities, and $\bar{Q}(\bar{\rho})$ becomes the self-organized linear relation

$$\bar{Q}(\bar{\rho}) = \frac{1}{T} \left(1 - \frac{\bar{\rho}}{\rho_{\text{jam}}} \right) \quad (4)$$

demanded by Kerner [16] [Figs. 1(a) and 2(b)]. T denotes the average time gap between the acceleration of successive vehicles. The linear relation (4) reflects a mixture of free and jammed traffic with characteristic densities ρ_{out} and ρ_{jam} , respectively, where the jammed regions grow with increasing density. $Q_{\text{out}} = \bar{Q}(\rho_{\text{out}})$ is the typical outflow from traffic jams [16]. The slope

$$C = \frac{\partial \bar{Q}}{\partial \bar{\rho}} = -\frac{1}{T \rho_{\text{jam}}} \quad (5)$$

corresponds to their dissolution velocity [16]. The dependence of the spatially averaged velocity \bar{V} on $\bar{\rho}$ is given by $\bar{V}(\bar{\rho}) = \bar{Q}(\bar{\rho}) / \bar{\rho}$. Regime III: In a parameter range $\lambda_{\max}(v_{\max}^1, p) < \lambda_1 < \lambda_{\text{stab}}(v_{\max}^1, p)$, there is still an unstable range of traffic, but $\bar{Q}(\bar{\rho})$ is piecewise linear with different slopes C and different values of ρ_{jam} or ρ_{out} [like in Fig. 1(b)], where the above relations are separately fulfilled for each linear piece. This may be understood as crossover behavior between the cases I and II. Notice that the discretization of vehicle dynamics implies $1/\rho_{\text{max}} = k_1 \Delta X$ and $T = k_2 \Delta T / k_3$ with small integers k_i (see below). Thus, C is restricted to a few discrete values $k_1 k_3 / k_2 \Delta V$. Regime IV:

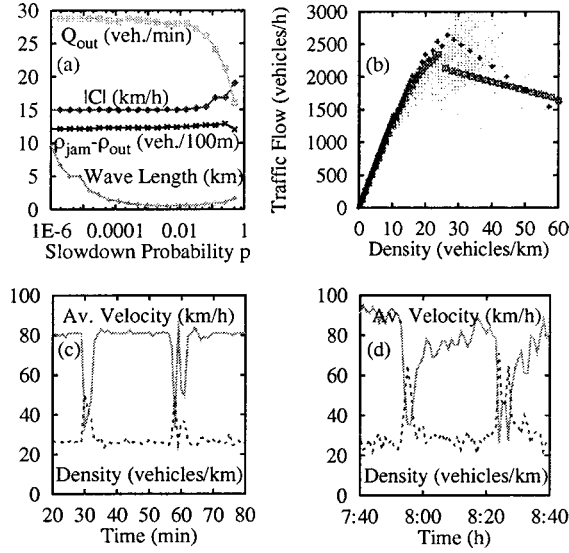


FIG. 2. (a) Characteristic parameters of traffic flow as a function of the slowdown probability p for the model parameters specified in Fig. 1. (b) Comparison of the model corresponding to $\lambda_a = 0.77$, $\rho = 0.001$, $\Delta T = 1$ s, $\Delta X = 2.5$ m, and the optimal flow relation specified by “+” with 1-minute-averages of single-vehicle data from the left lane of an undisturbed cross section of the Dutch highway A9 (\cdot). Boxes illustrate the simulated average flow resulting in the limit of long times. (c) Simulation of “stop-and-go waves” at an average density of 28 vehicles/km for a mixture of 90% cars and 10% trucks (the optimal velocities of which are only 70% of the cars). The occurring minimal and maximal velocities, the minimal densities, and the largely varying time intervals of successive breakdowns of velocity are in good agreement with the Dutch freeway data (1-minute-averages) displayed in (d). The mixture of vehicle types also explains the observed fluctuations in the density and average velocity of vehicles.

For $\lambda_1 v_{\max}^1 < 1$, λ_1 is so small that $v_{i+1}' \leq v_i$ which, for $p \neq 0$, implies that traffic eventually comes to rest.

The characteristic quantities can explicitly be calculated. Let us show this for the simple but nontrivial case $p \rightarrow 0$ and $v_1(d) = \min(d-1, 3)$ modeling city traffic. With $\Delta X = 6.25$ m we have $\rho_{\text{jam}} = 1/\Delta X = 160$ vehicles/km. Now, let us assume that a disturbance has produced a queue of vehicles with velocities $v = 0$ and distances $d = 1$ to the respective vehicles ahead, and a free road in front of the first vehicle. We can characterize the acceleration behavior of a vehicle by the sequence

$$(v_{i'}^*, d_{i'}) \rightarrow (v_{i'+1}^*, d_{i'+1}) \rightarrow (v_{i'+2}^*, d_{i'+2}) \rightarrow \dots, \quad (6)$$

where, for $\lambda = 0.77$, $v_{i+1} = \max(d_i - 2, 0)$ if $(v_i + 1) \leq d_i \leq 4$, and $d_{i+1} = (d_i + v_{i+1}^* - v_i)$ (v_{i+1}^* being the velocity of the vehicle ahead). Denoting with i' the time when the state $(0, 1)$ of the respective vehicle ahead has changed to another state, we find two alternating sequences: $(0, 1) \rightarrow (0, 1) \rightarrow (0, 3) \rightarrow (1, 4) \rightarrow (2, 4) \rightarrow (2, 4) \rightarrow \dots$ and $(0, 1) \rightarrow (0, 2) \rightarrow (0, 4) \rightarrow (2, 4) \rightarrow (2, 4) \rightarrow \dots$. That is, cars start to accelerate alternately every one or two time steps ΔT . With $\Delta T = 1$ s, we find an average of $T = 1.5$ s, which implies the dissolution velocity $C = -15$ km/h. Moreover, the resulting

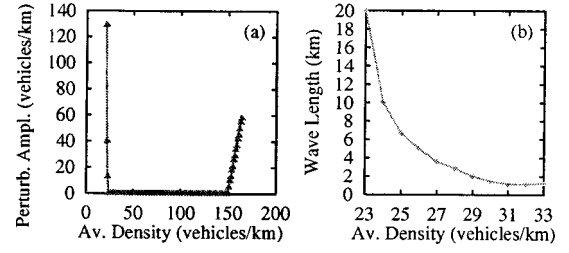


FIG. 3. (a) Critical amplitudes of localized perturbations with $w_+ = 200$ m and $w_- = 800$ m as a function of average density for the model specified in Fig. 2(b). Whereas larger perturbations cause the formation of traffic jams, smaller ones will fade away ($\rho_{c1} = 21$ vehicles/km, $\rho_{c2} = 23$ vehicles/km, $\rho_{c3} = 150$ vehicles/km, $\rho_{c4} \geq 164$ vehicles/km). (b) The average wave length of emerging stop-and-go waves diverges at ρ_{c2} (checked for large system sizes). This is why they are not triggered by fluctuations below this density.

density in front of jams is given by the evolving maximal distance $4\Delta X$, which gives $\rho_{\text{out}} = 40$ vehicles/km and, according to Eq. (4), an outflow of $Q_{\text{out}} = 1800$ vehicles/h. All this is in total agreement with simulation results [Fig. 1(a)].

Now, let us investigate the behavior for fixed $\lambda_1 = 0.77$ and density $\bar{\rho} = 80$ vehicles/km, but various p [Fig. 2(a)]. If p is continuously reduced, the backward dissolution velocity C is decreasing, whereas the outflow Q_{out} from traffic jams, and the difference between the jam density ρ_{jam} and the self-organized density ρ_{out} downstream of traffic jams are rapidly growing towards an almost constant value. In particular, the amplitude $(\rho_{\text{jam}} - \rho_{\text{out}})$ of traffic jams is constant over more than five decades.

In the deterministic case $p = 0$, the formation of traffic jams requires some initial inhomogeneity. Let us investigate the response to localized perturbations of the form

$$\rho(x, 0) = \bar{\rho} + \Delta\rho \{ \cosh^{-2}[(x - L/2)/w_+] - (w_+/w_-) \cosh^{-2}[(x - L/2 - w_+ - w_-)/w_-] \},$$

as suggested in Ref. [23]. Typically, one observes a piecewise linear response like in regime III [Fig. 1(b)]. However, its dependence on the perturbation amplitude $\Delta\rho$ indicates multistability, i.e., the coexistence of a variety of solutions. These correspond to periodic patterns of vehicle updates (which naturally result in deterministic systems with a *finite* number of states). In the presence of noise ($p > 0$), only one of them survives [Fig. 2(a)], i.e., most of them are unstable with respect to fluctuations. This explains the role of randomization for the behavior resulting in regime II.

Finally, let us focus on the density-dependent behavior for fixed $\lambda_1 = 0.77$ and $p > 0$. We find that initial localized perturbations of the above form, regardless of their amplitude $\Delta\rho$, are damped out for average densities $\bar{\rho}$ below some value $\rho_{c1}(v_{\max}^1, p)$ and above some value $\rho_{c4}(v_{\max}^1, p)$. In a certain density range $\rho_{c2}(v_{\max}^1, p) < \bar{\rho} < \rho_{c3}(v_{\max}^1, p)$, the perturbation grows for any finite amplitude. In the density regimes $\rho_{c1}(v_{\max}^1, p) \leq \bar{\rho} \leq \rho_{c2}(v_{\max}^1, p)$ and $\rho_{c3}(v_{\max}^1, p) \leq \bar{\rho} \leq \rho_{c4}(v_{\max}^1, p)$, we observe metastability [Fig. 3], i.e., perturbations with an amplitude $\Delta\rho \geq \Delta\rho_{\text{cr}}(\bar{\rho})$ will grow, other-

wise they will fade away in the course of time (“local cluster effect” [20,23]). Notice that $\rho_{c2} \approx \rho_{out}$ and $\rho_{c3} \approx \rho_{max}$.

These findings can be understood by analogy with the continuous optimal velocity model by Bando *et al.* [21] that results in the limit $\Delta T \rightarrow 0$ and $\Delta V \rightarrow 0$. It displays stable traffic at low and high vehicle densities, unstable traffic on the condition $dv_1(d)/dd > \lambda_1/2$, and metastable regimes between the unstable and stable ones [21]. However, in the *continuous* optimal velocity model, the jam density ρ_{jam} is not independent on how a traffic jam is formed, since fast cars are more crowded than slow ones, after they had to stop. This undesired property can be avoided by a refined model [24] or just by a suitable discretization, like in the proposed cellular automaton, when operated in regime II.

In summary, we have developed a cellular automaton for one-lane traffic which reproduces many of the empirically observed features of traffic flow in a “unified” way. In particular, the model showed the characteristic quantities of traffic flow, which we managed to calculate analytically. By appropriate specification of the tabular functions $v_a(d)$ and the parameters λ_a , p , ΔT , and ΔV , the model can be calibrated to empirical data. The most interesting case is to operate the model in regime II, since this guarantees the desired properties (iv) and (vi). The characteristic quantities like C

and Q_{out} are determined by ρ_{out} , $\rho_{jam} = k_1 \Delta T$, and $T = k_2 \Delta T / k_3$. The latter can be enforced by a suitable choice of ΔX and ΔT . $v_a(d)$ and λ_a determine the maximum velocity, the approximate velocity-density relation, the instability region, and the amplitude ($\rho_{jam} - \rho_{out}$) of traffic jams. The metastable regimes and the difference between the maximal possible traffic flow and the self-organized outflow Q_{out} from traffic jams grow with increasing v_{max}^a . Finally, p allows to influence the characteristic “wave length” between successive traffic jams [Fig. 2(a)]. Suitable choices are $\Delta T \in [1 \text{ s}, 1.3 \text{ s}]$, $\lambda_a \approx 0.77$ and $p \leq 0.01$. The optimal velocity functions $v_a(d)$ were chosen proportional to relations that were determined from traffic data of the Dutch freeway A9. The results are in good agreement with macroscopic traffic data [Figs. 2(b)–2(d)].

The authors acknowledge financial support by the BMBF (research project SANDY) and the DFG (Heisenberg Contract No. He 2789/1-1). They are grateful to B. Kerner for valuable comments, and to H. Taale and the Dutch Ministry of Transport, Public Works and Water Management for supplying the freeway data.

-
- [1] S. Wolfram, *Nature (London)* **311**, 419 (1984).
 - [2] P. Bak *et al.*, *Phys. Rev. Lett.* **59**, 381 (1987).
 - [3] P. Bantay and I.M. Janosi, *Phys. Rev. Lett.* **68**, 2058 (1992).
 - [4] Z. Olami *et al.*, *Phys. Rev. Lett.* **68**, 1244 (1992).
 - [5] M. Markus and B. Hess, *Nature (London)* **347**, 56 (1990).
 - [6] M.A. Nowak and R.M. May, *Nature (London)* **359**, 826 (1992).
 - [7] G. Peng and H.J. Herrmann, *Phys. Rev. E* **49**, R1796 (1994).
 - [8] U. Frisch *et al.*, *Phys. Rev. Lett.* **56**, 1505 (1986); S. Chen *et al.*, *ibid.* **67**, 3776 (1991).
 - [9] D. Dab *et al.*, *Phys. Rev. Lett.* **66**, 2535 (1991).
 - [10] K. Nagel and M. Schreckenberg, *J. Phys. I* **2**, 2221 (1992); M. Schreckenberg *et al.*, *Phys. Rev. E* **51**, 2939 (1995).
 - [11] T. Nagatani, *Phys. Rev. E* **51**, 922 (1995).
 - [12] *Traffic and Granular Flow '97*, edited by M. Schreckenberg and D.E. Wolf (Springer, Singapore, 1998).
 - [13] D. Helbing, *Traffic Dynamics* (Springer, Berlin, 1997) (in German).
 - [14] D. Helbing and M. Treiber, *Phys. Rev. Lett.* **81**, 3042 (1998).
 - [15] B.S. Kerner and H. Rehborn, *Phys. Rev. E* **53**, R1297 (1996); **53**, R4275 (1996).
 - [16] B.S. Kerner, in *Transportation Systems*, edited by M. Papageorgiou and A. Pouliezios (International Federation of Automatic Control, Chania, Greece, 1997), Vol. II.
 - [17] K. Nagel and H.J. Herrmann, *Physica A* **199**, 254 (1993); M. Takayasu and H. Takayasu, *Fractals* **1**, 860 (1993).
 - [18] S. Krauß *et al.*, *Phys. Rev. E* **54**, 3707 (1996); **55**, 5597 (1997); S. Krauß, *Microscopic Modelling of Traffic Flow* (DLR, Cologne, 1998), FB 98-08.
 - [19] B. Barlovic *et al.*, *Eur. Phys. J. B* **5**, 793 (1998).
 - [20] B.S. Kerner and P. Konhäuser, *Phys. Rev. E* **48**, R2335 (1993); **50**, 54 (1994).
 - [21] M. Bando *et al.*, *Phys. Rev. E* **51**, 1035 (1995) and *J. Phys. I* **5**, 1389 (1995).
 - [22] D. Helbing and B.A. Huberman, *Nature (London)* **396**, 738 (1998).
 - [23] M. Herrmann and B.S. Kerner, *Physica A* **255**, 163 (1998).
 - [24] D. Helbing and B. Tilch, *Phys. Rev. E* **58**, 133 (1998).